

# Optimization of Electrochemical and Peroxide-Driven Oxidation of Styrene with Ultrathin Polyion Films Containing Cytochrome P450<sub>cam</sub> and Myoglobin

Bernard Munge,<sup>[a]</sup> Carmelita Estavillo,<sup>[a]</sup> John B. Schenkman,<sup>[b]</sup> and James F. Rusling<sup>\*[a, b]</sup>

*The catalytic and electrochemical properties of myoglobin and cytochrome P450<sub>cam</sub> in films constructed with alternate polyion layers were optimized with respect to film thickness, polyion type, and pH. Electrochemical and hydrogen peroxide driven epoxidation of styrene catalyzed by the proteins was used as the test reaction. Ionic synthetic organic polymers such as poly(styrene sulfonate), as opposed to SiO<sub>2</sub> nanoparticles or DNA, supported the best catalytic and electrochemical performance. Charge transport involving the iron heme proteins was achieved over 40–320 nm depending on the polyion material and is likely to involve electron hopping facilitated by extensive interlayer mixing. However, very*

*thin films (ca. 12–25 nm) gave the largest turnover rates for the catalytic epoxidation of styrene, and thicker films were subject to reactant transport limitations. Classical bell-shaped activity/pH profiles and turnover rates similar to those obtained in solution suggest that films grown layer-by-layer are applicable to turnover rate studies of enzymes for organic oxidations. Major advantages include enhanced enzyme stability and the tiny amount of protein required.*

## KEYWORDS:

cytochromes · electrolysis · epoxidation · metalloenzymes · thin films

## Introduction

A powerful and general method for layer-by-layer construction of ultrathin enzyme films held together by a polyion “glue” emerged during the 1990s.<sup>[1–3]</sup> To illustrate the approach, first consider an enzyme in a buffer with a pH value less than its isoelectric point, so that the enzyme has a positive surface charge. A solid surface with an adsorbed layer of polyanions, such as poly(styrene sulfonate) (PSS), is immersed into this solution, and a layer of enzyme is adsorbed. For appropriate enzyme concentrations (usually 1–3 mg mL<sup>−1</sup>), cationic amino acid residues are exposed at the interface with the solution after adsorption. The surface charge on the solid is altered to that of the new outer layer, being effectively reversed in this case. This solid is washed with water, then immersed into a polyanion solution, in which a new layer is adsorbed, returning the surface to the negative charge. Repetition of these cycles of enzyme and polyion adsorption alternately with intermediate washing provides multilayer films with reproducible amounts of enzyme in each layer and nanometer-scale control of thickness. If the enzyme is negatively charged, polycations are used for the alternating layers. The technique provides stable films and facilitates increases in the loading of enzyme per unit surface area by increasing the number of layers.

More than 20 enzymes and proteins have been incorporated into films by this electrostatic layer-by-layer self-assembly technique.<sup>[2, 3]</sup> Synthetic polyions, metal oxide nanoparticles,

and biological polyions such as DNA have been used to alternate with the enzyme layers.<sup>[2–5]</sup> In general, enzymes retain their native structures and activities in these films and can be used for catalysis. Films of a few enzyme/polyion bilayers contain only tiny amounts of enzyme, often considerably less than 10 nmol. The method is also amenable to the incorporation of several enzymes in films for sequential catalytic reactions.<sup>[3, 4]</sup>

Several years ago, our group was the first to achieve reversible electron exchange with metalloproteins in such films on electrodes.<sup>[6]</sup> We constructed layered films of myoglobin (Mb) and cytochrome P450<sub>cam</sub> (cyt P450<sub>cam</sub>) with polyions and employed them for enzyme catalysis, driven either electrochemically or by addition of hydrogen peroxide.<sup>[6–9]</sup> Cyt P450<sub>cam</sub> and Mb were used in these films to epoxidize styrene and *cis*-methyl styrene. The electrochemical catalytic processes is initiated by

[a] Prof. J. F. Rusling, B. Munge, C. Estavillo  
Department of Chemistry, U-60  
University of Connecticut  
Storrs, Connecticut 06269-3060 (US)  
Fax: (+1) 860-486-2981  
E-mail: James.Rusling@uconn.edu

[b] Prof. J. F. Rusling, Prof. J. B. Schenkman  
Department of Pharmacology  
University of Connecticut Health Center  
Farmington, Connecticut 06032 (US)

reversible electrochemical conversion of heme  $\text{Fe}^{\text{III}}/\text{Fe}^{\text{II}}$  in the protein films. The  $\text{Fe}^{\text{II}}$  enzyme binds dioxygen and this complex is electrochemically reduced to give hydrogen peroxide, which subsequently mediates the enzyme-catalyzed oxidations of organic reactants. The key activating role of hydrogen peroxide was confirmed by the absence of products in the presence of catalase, which destroyed all the hydrogen peroxide. Human cyt P450 3A4 in films on electrodes converted the drugs verapamil and midazolam into their expected liver metabolites in peroxide-dependent electrochemical processes.<sup>[10]</sup> Using a quartz crystal microbalance and atomic force microscopy, we recently found that cyt P450s orient specifically on polyion layers.<sup>[11]</sup>

These early results suggested that electrostatic layer-by-layer self-assembly of enzyme films may be a promising new alternative for traditional enzymology studies, as well as for biosensor and bioreactor fabrication. Major advantages include improved enzyme stability and the tiny amounts of enzyme used. For membrane-bound enzymes such as mammalian cyt P450s,<sup>[12, 13]</sup> catalytic reactions in these films mimic nature by having the enzymes bound to a surface. The films facilitate reasonably fast and reversible heme  $\text{Fe}^{\text{III}}/\text{Fe}^{\text{II}}$  conversion of the enzymes, which allows catalytic reactions to be driven electrochemically.<sup>[7–9]</sup> This cannot be done efficiently with enzymes dissolved in solution because of very slow  $\text{Fe}^{\text{III}}/\text{Fe}^{\text{II}}$  conversion at electrodes.

Our earlier papers on catalysis with heme enzymes in layer-by-layer polyion films<sup>[6, 7, 10]</sup> employed a single pH value and films containing one or two enzyme/polyion bilayers. In this paper, in order to establish optimum conditions for construction and use of these films, we evaluate the influence of the number of enzyme layers (i.e., film thickness), the nature of the alternating polyion, and the effect of the pH value of the reaction buffer on turnover rates in these multilayer films. We employed the epoxidation of styrene catalyzed by cyt P450<sub>cam</sub> and Mb as a test reaction. Catalyst turnover rate was controlled by film thickness, the pH value of the external solution, and the type of polyion used.

## Results

### Film assembly and characterization

Films of Mb with PSS, DNA, and  $\text{SiO}_2$  nanoparticles (45 nm diameter) and films of cyt P450<sub>cam</sub> with poly(ethyleneimine) (PEI) were used in this work. They are denoted (protein/polyion)<sub>n</sub>, where *n* is the number of protein/polyion bilayers. The term "(Mb/PSS, 0.5 M NaCl)<sub>2</sub>" indicates that PSS was adsorbed from 0.5 M NaCl, which coils PSS to give thicker films.<sup>[6]</sup> Construction of the films on quartz crystal microbalance (QCM) resonators was used to monitor the quality of film formation.<sup>[2, 3, 8, 9]</sup> The Sauerbrey equation gives the relation between adsorbed mass and frequency shift  $\Delta F$  (Hz) of the quartz resonator. For 9-MHz quartz resonators the film mass per unit area  $M/A$  ( $\text{g cm}^{-2}$ ) for our resonators of  $A = 0.16 \pm 0.01 \text{ cm}^2$  on one side is given by Eq. (1):<sup>[14]</sup>

$$\frac{M}{A} = \frac{-\Delta F}{(1.83 \times 10^8)} \quad (1)$$

The nominal thickness (*d*) of dry films can be estimated from Eqn. (2), confirmed by high-resolution scanning electrochemical microscopy cross-sections:<sup>[2, 3, 14]</sup>

$$d(\text{nm}) = -(0.016 \pm 0.002)\Delta F(\text{Hz}) \quad (2)$$

QCM monitoring of film formation is illustrated for (cyt P450<sub>cam</sub>/PEI)<sub>n</sub> films. Reproducible decreases in  $\Delta F$  were observed as adsorbed layers were added to the film (Figure 1),

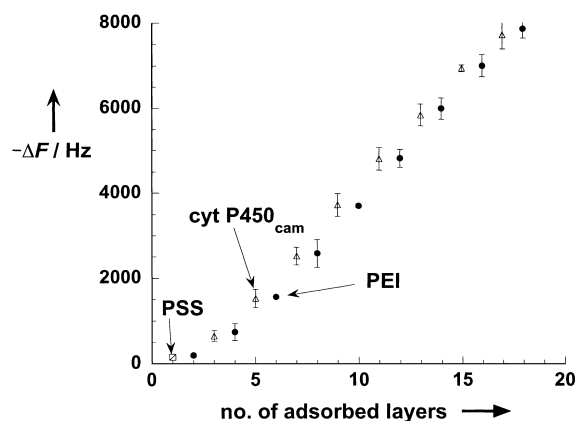


**Figure 1.** QCM frequency changes as a function of the number of adsorbed layers during monitoring of the growth of (cyt P450<sub>cam</sub>/PEI)<sub>n</sub> films on gold resonators.

which indicates regular and reproducible layer formation. The  $\Delta F$  values<sup>[5, 6]</sup> together with Eqs. (1) and (2) gave the following nominal average thicknesses and amounts of proteins for bilayers on gold: (Mb/PSS, 0.5 M NaCl) = 12 nm,  $2 \times 10^{-10} \text{ mol cm}^{-2}$ ; (Mb/PSS) = 6 nm,  $1.1 \times 10^{-10} \text{ mol cm}^{-2}$ ; (Mb/ $\text{SiO}_2$ ) = 40 nm,  $1.7 \times 10^{-10} \text{ mol cm}^{-2}$ ; (Mb/DNA) = 7 nm,  $1 \times 10^{-10} \text{ mol cm}^{-2}$ ; (cyt P450<sub>cam</sub>/PEI) = 15 nm,  $1 \times 10^{-10} \text{ mol cm}^{-2}$ . Film thicknesses and total amount of protein are obtained by multiplying these bilayer values by *n*.

Cyclic voltammograms (CVs) were obtained after each bilayer adsorption cycle during assembly of protein/polyion films on rough pyrolytic graphite (PG) electrodes. Well-defined chemically reversible CV peaks similar to those reported previously<sup>[6, 9]</sup> were observed, as illustrated for (cyt P450<sub>cam</sub>/PEI)<sub>n</sub> in Figure 2. Here, all the electrochemically active  $\text{Fe}^{\text{III}}$  enzyme is reduced on the forward scan, and the  $\text{Fe}^{\text{II}}$  enzyme is oxidized on the reverse scan. Peak currents varied linearly with scan rate from 0.05 to  $2.0 \text{ V s}^{-1}$  for both Mb and cyt P450<sub>cam</sub> films, but had nonzero peak separations and peak widths exceeding the ideal 90 mV, consistent with nonideal thin layer electrochemistry.<sup>[9, 15]</sup>

The charge (*Q*) obtained by integration of forward-scan voltammograms for one-electron reduction of the  $\text{Fe}^{\text{III}}$  proteins is related to the amount of electroactive protein per unit electrode area ( $\Gamma_T$ ) by Equation (3):<sup>[9]</sup>

$$Q = FA\Gamma_T \quad (3)$$

where *F* is Faraday's constant and *A* is electrode area.  $\Gamma_T$  increased with increasing number of protein/polyion bilayers (Figure 3) and depended on the type of polyion. For (Mb/PSS)<sub>n</sub>,

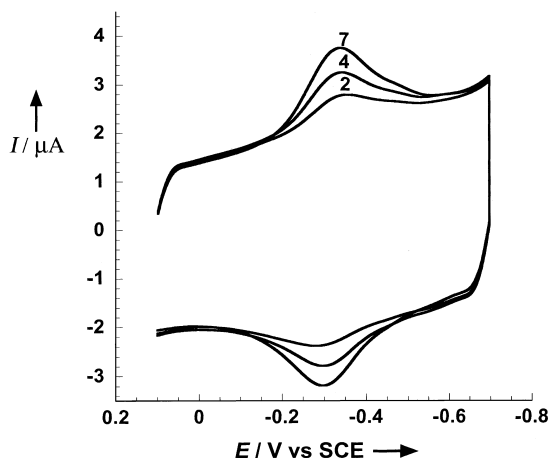


**Figure 2.** Cyclic voltammograms at  $0.3 \text{ V s}^{-1}$  for (cyt P450cam/PEI) $_n$  on rough PG electrodes in acetate (50 mM, pH 5.5) + NaCl (100 mM) purged with nitrogen. The numbers on the curves denote  $n$ .

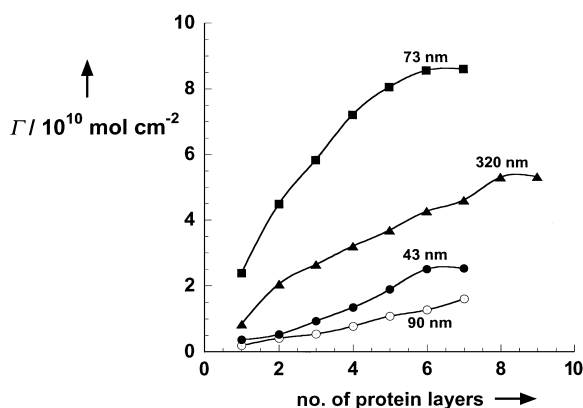


**Figure 3.** Influence of number of protein layers ( $n$ ) on amount of electroactive protein ( $\Gamma$ ) for (Mb/PSS) $_n$  (■), (Mb/SiO $_2$ ) $_n$  (▲), (Mb/DNA) $_n$  (●), and (cyt P450cam/PEI) $_n$  (○) films, measured by CV at  $0.3 \text{ V s}^{-1}$  at pH 5.5. The numbers near data points are film thicknesses estimated from QCM results for the given  $n$  value.

(Mb/DNA) $_n$  saturation was achieved at  $n = 7$ . For (Mb/SiO $_2$ ) $_n$ , electroactivity extended up to  $n = 8$ , which represents electron transport across a 320-nm thick film. For (cyt P450cam/PEI) $_n$ , increases in  $\Gamma_T$  were found up to  $n = 7$ . For all films, CV scans were reproducible and films were stable in buffer for at least two weeks.

### Influence of pH on voltammetry

CV peaks for Mb and cyt P450cam films shifted to negative potentials with increasing pH value, as illustrated for Mb (Figure 4).  $\Gamma_T$  values for (protein/polyion) $_6$  films were essentially constant between pH 3.0 and pH 11, with average values of: (Mb/PSS, 0.5 M NaCl) $_6$ ,  $8.5 \pm 0.2 \times 10^{-10} \text{ mol cm}^{-2}$ ; (Mb/SiO $_2$ ) $_6$ ,  $5.2 \pm 0.2 \times 10^{-10} \text{ mol cm}^{-2}$ ; (Mb/DNA) $_6$ ,  $2.4 \pm 0.1 \times 10^{-10} \text{ mol cm}^{-2}$ ; (cyt P450cam/PEI) $_6$ ,  $1.8 \pm 0.2 \times 10^{-10} \text{ mol cm}^{-2}$ . Division of these values by the total mass of protein in each film estimated by QCM gave the following percentages of electroactive protein in each film: (Mb/PSS, 0.5 M NaCl) $_6$ , 70%; (Mb/SiO $_2$ ) $_6$ , 50%; (Mb/DNA) $_6$ , 40%; and (cyt P450cam/PEI) $_6$ , 30%. All

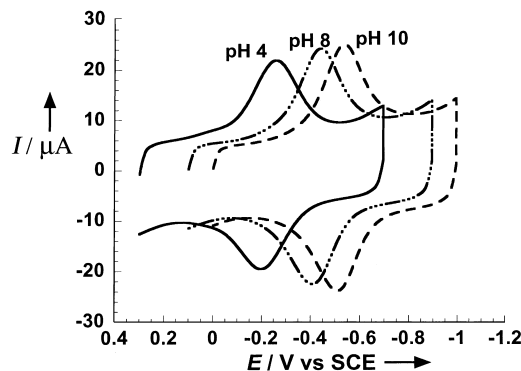


**Figure 4.** Cyclic voltammograms at  $0.3 \text{ V s}^{-1}$  for (Mb/PSS) $_6$  film on PG electrode at several pH values (buffers + 100 mM NaCl and purged with nitrogen).

changes in CV peak shapes and potentials were reversible for both Mb and cyt P450cam films. For example, CVs for Mb and cyt P450cam films at pH 7 were reproduced after immersion of the films in pH 3 buffer and then returning of the films to the pH 7 buffer.

Formal potentials ( $E^{\circ'}$ ) of the heme Fe<sup>III</sup>/Fe<sup>II</sup> redox couples of Mb and cyt P450cam in the films were estimated as the midpoint between CV reduction and oxidation peak potentials. All  $E^{\circ'}$  values were linear at pH values over the pH range 3–11 (Figure 5). Average slopes in mV pH<sup>-1</sup> were: (Mb/PSS) $_6$ , -49; (Mb/DNA) $_6$ , -48; (Mb/SiO $_2$ ) $_6$ , -50; (cyt P450cam/PEI) $_6$ , -45. These slopes are slightly smaller than the theoretical value of

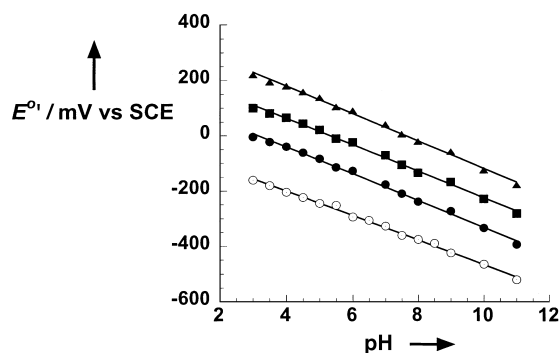


**Figure 5.** Influence of pH value on formal potential ( $E^{\circ'}$ ) obtained from CV at  $0.3 \text{ V s}^{-1}$  for (Mb/PSS) $_6$  (●), (Mb/SiO $_2$ ) $_6$  (▲), (Mb/DNA) $_6$  (■), and (cyt P450cam/PEI) $_6$  (○) films on PG electrodes (buffers + 100 mM NaCl and purged with nitrogen).

$-59 \text{ mV pH}^{-1}$  at  $25^\circ\text{C}$  for a reversible one-electron transfer coupled to proton transfer during electrochemical reduction.<sup>[16]</sup> Reduction and oxidation peak separations ( $\Delta E_p$ ), which are inversely related to the efficiency of electron transfer in the films<sup>[9]</sup> and are also influenced by redox-coupled conformational changes,<sup>[17]</sup> were at a maximum between pH 4 and 6 and decreased to constant values at pH > 8.5 (Figure 6).

### Catalytic activity for oxidation of styrene

The oxidation of styrene to styrene oxide can be catalyzed by cyt P450cam and Mb in solution<sup>[18, 19]</sup> and by use of films on

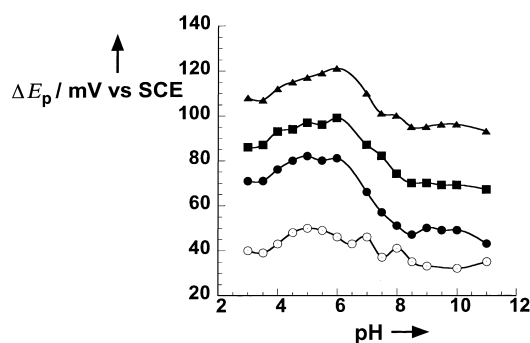
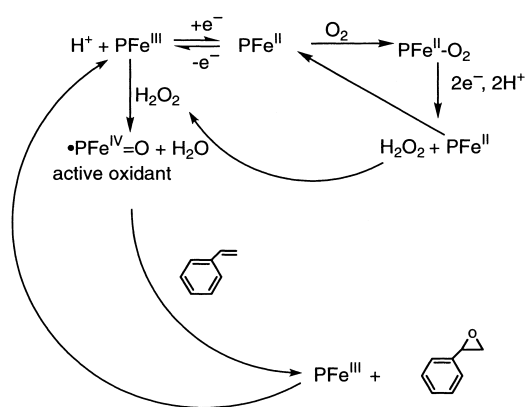


**Figure 6.** Influence of pH value on separation of reduction and oxidation peak potentials ( $\Delta E_p$ ) from CV at  $0.3 \text{ V s}^{-1}$  for  $(\text{Mb}/\text{PSS})_6$  (●),  $(\text{Mb}/\text{SiO}_2)_6$  (■),  $(\text{Mb}/\text{DNA})_6$  (▲), and  $(\text{cyt P450}_{\text{cam}}/\text{PEI})_6$  (○) films on PG electrodes.

electrodes.<sup>[6, 7]</sup> Scheme 1 shows that the reaction can be accomplished either by an electrochemical pathway producing  $\text{H}_2\text{O}_2$ , or driven by addition of  $\text{H}_2\text{O}_2$  without electrolysis.



**Scheme 1.** Suggested pathway for electrochemical and chemical catalysis of styrene epoxidation with iron heme proteins (PFe).

In films on electrodes, the  $\text{PFe}^{\text{II}}/\text{O}_2$  complex is formed after  $\text{PFe}^{\text{III}}$  is reduced in the presence of oxygen. Electrochemical reduction of  $\text{PFe}^{\text{II}}/\text{O}_2$  gives hydrogen peroxide at the  $\text{Fe}^{\text{III}}/\text{Fe}^{\text{II}}$  redox potential. This catalytic reduction can be detected by CV as an increase in reduction current in the presence of oxygen (Figure 7) and the disappearance of the oxidation peak for  $\text{PFe}^{\text{II}}$ , consistent with its fast reaction with oxygen. An increase in the amount of oxygen in the buffer increased the height of the catalytic reduction peak because of the increased reaction rate. The catalytic reduction is approximately 0.5 V more positive than direct reduction of oxygen (Figure 7). Catalytic efficiency, expressed as  $I_c/I_d$ , the ratio of reduction peak currents in the presence ( $I_c$ ) and absence ( $I_d$ ) of oxygen, was optimum for two protein layers, as illustrated for  $(\text{Mb}/\text{PSS})_n$  in Figure 8.

All turnover studies were done at  $4^\circ\text{C}$  to protect the proteins from damage from hydrogen peroxide.<sup>[7]</sup> Gas chromatography shows that the product of the enzyme-catalyzed process is styrene oxide, while benzaldehyde is a product of the reaction of styrene with  $\text{H}_2\text{O}_2$ .<sup>[7, 19]</sup> As illustrated for  $(\text{Mb}/\text{PSS}, 0.5 \text{ M NaCl})$  films, turnover rates from the electrolyses decreased with

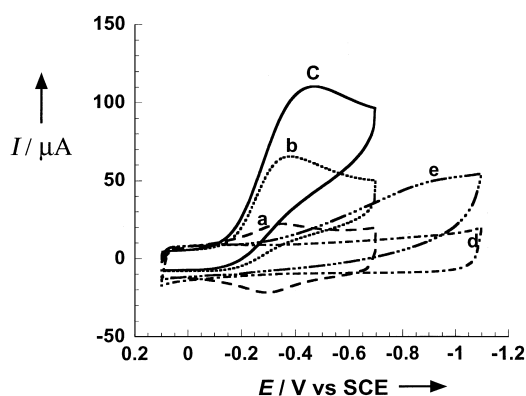


**Figure 7.** Cyclic voltammograms at  $0.3 \text{ V s}^{-1}$  in pH 5.5 buffer in a sealed cell for: a)  $(\text{cyt P450}_{\text{cam}}/\text{PEI})_6$  film with no oxygen present, b)  $(\text{cyt P450}_{\text{cam}}/\text{PEI})_6$  film after injection of 20 mL oxygen into the buffer, c)  $(\text{cyt P450}_{\text{cam}}/\text{PEI})_6$  after injection of 40 mL oxygen, d) PEI monolayer on PG without oxygen present, and e) PEI monolayer after injection of 40 mL oxygen.

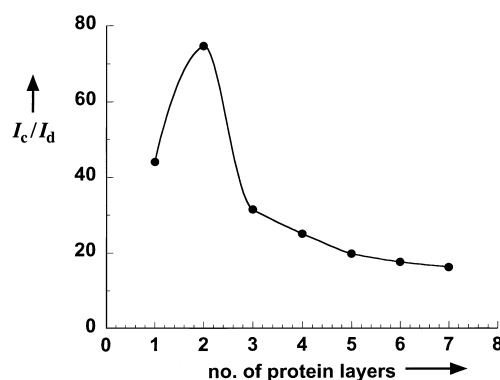


**Figure 8.** Influence of film thickness on catalytic efficiency,  $I_c/I_d$ , for  $(\text{Mb}/\text{PSS})_n$  ( $n = 1.7$ ) films in buffer (4 mL, pH 5.5), where  $I_d$  is the CV reduction peak current in buffer without oxygen and  $I_c$  is the CV reduction peak current after injection of 40 mL oxygen into the buffer in a sealed cell.

increasing number of protein layers and film thickness (Table 1). The turnover rate decreased between one and four protein layers and then leveled out for five and six protein layers. The mass yields for styrene oxide, however, increased with film thickness to a maximum at 49 nm (four bilayers), then decreased as film thickness increased further. Amounts of  $\text{H}_2\text{O}_2$  found after 1 hr were relatively unaffected by film thickness.

In view of the thickness dependence described above, all further experiments were done with two protein layers. The effect of polyion type was examined at neutral pH. PSS was deposited from water with no added salt to achieve thinner films and higher turnover rates. To illustrate this effect, the turnover rate for 25 nm thick  $(\text{Mb}/\text{PSS}, 0.5 \text{ M NaCl})_2$  was  $2 \text{ hr}^{-1}$  (Table 1), while that of 13 nm  $(\text{Mb}/\text{PSS})_2$  deposited without use of salt was  $3.9 \text{ hr}^{-1}$ . Amongst the three different Mb films,  $(\text{Mb}/\text{PSS})_2$  gave the best catalytic efficiency for both electrochemical and  $\text{H}_2\text{O}_2$  driven oxidation of styrene. The  $\text{H}_2\text{O}_2$  driven oxidation with  $(\text{Mb}/\text{PSS})_2$  gave the highest turnover rate at  $7.4 \text{ hr}^{-1}$ . Similar mass yields of styrene oxide were found for the electrochemically enzyme driven catalysis when using either  $(\text{Mb}/\text{PSS})_2$  or  $(\text{cyt P450}_{\text{cam}}/\text{PEI})_2$  films, but  $\text{cyt P450}_{\text{cam}}$  gave the best turnover rate

**Table 1.** Influence of the thickness of a (Mb/PSS, 0.5 M NaCl)<sub>n</sub> film on a carbon cloth cathode on the electrochemical catalytic activity for styrene epoxidation.<sup>[a]</sup>

nominal thickness (n) [nm]	Amount protein [nmol]	Styrene oxide found [nmol]	Benzaldehyde found [nmol]	Turnover rate [hr <sup>-1</sup> ] <sup>[b]</sup>	[H <sub>2</sub> O <sub>2</sub> ] found [mM]
13 (1)	8.7	30.6 ± 0.4	30.3 ± 0.2	3.5	10
25 (2)	15.7	31.7 ± 0.7	24.9 ± 1.0	2.0	10
37 (3)	25.9	39.9 ± 3.6	35.5 ± 1.3	1.5	10
49 (4)	36.1	49.4 ± 0.5	37.2 ± 0.5	1.4	10
61 (5)	45.1	25.3 ± 1.3	15.7 ± 0.8	0.6	9
73 (6)	52.6	38.0 ± 1.5	26.0 ± 0.8	0.7	9
Control, PSS	0	1.4 ± 0.3	3.5 ± 0.6	-	3

[a] Product yields were determined by GC. Oxygen was bubbled through the reactor for 20 min before and at the beginning of each experiment, followed by oxygen blanketing throughout the 1-hr electrolysis period. Applied potential: -0.6 V vs. SCE at 4 °C. Buffer: 50 mM Tris + 50 mM NaCl, pH 7.4. [b] Turnover rate was measured as moles styrene reacted per mole Mb per hour.

(6.3 hr<sup>-1</sup>). To put this value into context, we performed a solution assay of styrene oxidation at 4 °C with cyt P450<sub>cam</sub> and with putidaredoxin with NADH as electron donor and obtained a turnover rate of 10 hr<sup>-1</sup>.

In all electrolyses with protein present, the amount of hydrogen peroxide found was significantly higher than seen in the control experiments with no protein (compare Table 1 and Table 2). In all the films studied, styrene oxidation for 1 hr by aerobic electrolysis at 4 °C resulted in decomposition of roughly 20% of the protein, as estimated by voltammetry.

The influence of the pH value of the external buffer on turnover rate was investigated for (Mb/PSS)<sub>2</sub>, (Mb/SiO<sub>2</sub>)<sub>2</sub>, and (cyt P450<sub>cam</sub>/PEI)<sub>2</sub>. Activity/pH profiles for Mb films were different, depending on whether the reaction was driven by electrolysis or by H<sub>2</sub>O<sub>2</sub> addition (Figure 9). For electrolyses, an increase in the pH resulted in a decrease in the turnover rate for styrene oxidation, but this was correlated with the amount of hydrogen peroxide formed (numbers beside points). On the other hand, addition of hydrogen peroxide at 10 mM produced an activity/pH profile with a maximum in the physiological pH range.

Electrolytic and H<sub>2</sub>O<sub>2</sub> driven epoxidations of styrene with (cyt P450<sub>cam</sub>/PEI)<sub>2</sub> films gave activity/pH profiles of similar shapes (Figure 10). In this case, 10 mM H<sub>2</sub>O<sub>2</sub> was found at the end of the 1 hr electrolyses at all pH values. The electrolytic turnover rates were slightly larger than the peroxide-driven values.

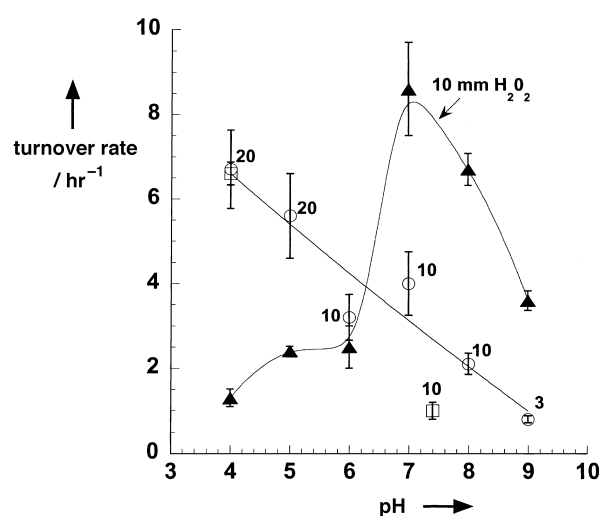


**Figure 9.** Influence of pH value on turnover rate as moles styrene oxide per mole protein per hour for 1-hr reactions at 4 °C for oxidation of styrene to styrene oxide catalyzed by (Mb/PSS)<sub>2</sub> films on carbon cloth electrodes by electrolysis (○) or by addition of 10 mM H<sub>2</sub>O<sub>2</sub> (▲), and by (Mb/SiO<sub>2</sub>)<sub>2</sub> films by electrolysis (□). The electrolysis potential was -0.6 V vs. SCE at 4 °C and oxygen was bubbled through the reaction mixture for the first 20 min of electrolysis. H<sub>2</sub>O<sub>2</sub> mediated reactions were performed under an atmosphere of air. The numbers above the data points for electrolysis results represent amount (mM) H<sub>2</sub>O<sub>2</sub> found at the end of the 1-hr reaction. Controls run in the absence of Mb at all pH values gave 1–10% of the amount of styrene oxide found in the catalytic reactions.

**Table 2.** Effect of polyion type on catalytic activity for styrene epoxidation.

Film	Amount protein [nmol]	Styrene oxide found <sup>[a]</sup> [nmol]	Benzaldehyde found <sup>[a]</sup> [nmol]	Turnover Rate <sup>[b]</sup> [hr <sup>-1</sup> ]	[H <sub>2</sub> O <sub>2</sub> ] found [mM]
<b>Electrolyses:</b>					
PSS(Mb/PSS) <sub>2</sub>	5.8	22.7 ± 0.6	23.1 ± 1.8	3.9	10
DNA(Mb/DNA) <sub>2</sub>	4.2	8.0 ± 1.7	8.9 ± 1.5	1.9	6
PSS/PDDA/SiO <sub>2</sub> (Mb/SiO <sub>2</sub> ) <sub>2</sub>	3.7	3.7 ± 0.3	6.7 ± 0.9	1.0	10
PEI(cyt P450 <sub>cam</sub> /PEI) <sub>2</sub>	1.6	10.2 ± 0.1	15.3 ± 3.6	6.3	10
<b>Control electrolyses:</b>					
PSS	0	1.4 ± 0.3	3.5 ± 0.6		3
PEI	0	1.4 ± 0.2	3.5 ± 0.6		3
DNA	0	1.1 ± 0.1	2.2 ± 0.4		3
PSS/PDDA <sup>[c]</sup> /SiO <sub>2</sub>	0	0.8 ± 0.1	2.4 ± 0.4		3
<b>Chemical reactions:<sup>[b]</sup></b>					
PSS(Mb/PSS) <sub>2</sub> + 10 mM H <sub>2</sub> O <sub>2</sub>	5.8	43.1 ± 6.2	10.2 ± 2.5	7.4	10
PSS + 10 mM H <sub>2</sub> O <sub>2</sub> (control)	0	2.0 ± 0.3	1.5 ± 0.2		10

[a] Products determined by GC for reactions carried out at 4 °C at pH 7.4 by electrolysis at -0.6 vs. SCE under oxygen (see Table 1) or by addition of H<sub>2</sub>O<sub>2</sub> under air. Buffer: 50 mM Tris + 50 mM NaCl. [b] As defined in Table 1. [c] PDDA = polydimethyldiallylammonium chloride.

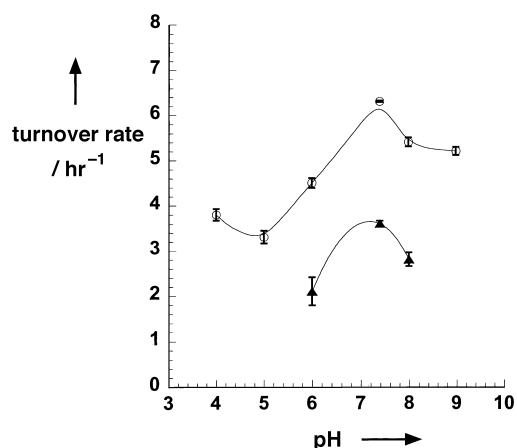


**Figure 10.** Influence of pH value on turnover rate as moles styrene oxide per mole protein per hour for 1-hr reactions at 4 °C for oxidation of styrene to styrene oxide catalyzed by (cyt P450<sub>cam</sub>/PEI)<sub>2</sub> films on carbon cloth electrodes by electrolysis (○) or by addition of 10 mM H<sub>2</sub>O<sub>2</sub> (▲). The electrolysis potential was −0.6 V vs. SCE at 4 °C and oxygen was bubbled through the reaction mixture for the first 20 min of electrolysis. H<sub>2</sub>O<sub>2</sub> mediated reactions were performed under an atmosphere of air. Electrolyses at all pH values gave 10 mM H<sub>2</sub>O<sub>2</sub> at the end of the 1-hr reaction. Controls run without enzyme at all pH values gave 10–30% of the amount of styrene oxide found in the catalytic reactions.

## Discussion

### Influence of polyion materials

The above results show that the electrochemical and catalytic activity of films of heme proteins made by the layer-by-layer electrostatic method depend on the polyion used in the assembly procedure, on film thickness, and on pH conditions. Data for Mb constructed with SiO<sub>2</sub>, PSS, and DNA as the polyion show that all films gave chemically reversible electron transfer for Fe<sup>III</sup>/Fe<sup>II</sup> (Figures 2 and 4). However, the type of polyion influenced the amount of protein incorporated into the film (Figure 3), the fraction of protein that is electroactive, and the redox potential (Figure 5). For example, (Mb/PSS)<sub>6</sub> films had the most negative formal potentials among the Mb films, but contained the largest amount of protein, and 70% of the Mb was electroactive. About half of the Mb in DNA and SiO<sub>2</sub> films of six bilayers was electroactive, and only 30% cyt P450cam was electroactive in six-bilayer films with PEI.

It has been observed before for other types of metalloprotein films that the redox potential in general depends on film composition, and this was attributed to protein–film interactions and electrode double-layer effects.<sup>[9]</sup> The polyion material used here also influenced catalytic activity, with the best turnover rates for styrene epoxidation being obtained for films made with synthetic polyions, rather than DNA or SiO<sub>2</sub> (Table 2). Lower yields in DNA films may be related to the reaction of styrene oxide with guanine and adenine bases in the DNA in the films.<sup>[20]</sup>

### Influence of film thickness

Voltammetry showed that electron transfer extends out to six or more layers of protein for all the films built on rough PG

(Figures 2 and 3). Charge transport involving the iron heme proteins was achieved over 40 nm for (Mb/DNA)<sub>6</sub> and 320 nm for (Mb/SiO<sub>2</sub>)<sub>8</sub> in the various films, and is likely to involve electron hopping facilitated by extensive interlayer mixing. We previously suggested that the roughness of the electrode acts as a disordering template, which facilitates overlap of the layers in the film<sup>[21]</sup> and brings protein molecules closer together (estimated 4–6 nm average inter-heme distances) so that they can participate in an electron hopping pathway. Even on smooth surfaces, extensive mixing of neighboring layers was demonstrated by neutron reflectance analysis in films of PSS and polycations, and PSS and Mb.<sup>[3, 22]</sup> Thus, although the films are constructed one layer at a time, the final structure features considerable intermixing, which facilitates charge transport through the film.

Voltammetric catalytic efficiency data for reduction of oxygen (Figure 8) and turnover rates for epoxidation of styrene (Table 1) are consistent with the onset of reactant mass transport limitations as the films get thicker. An increase in the number of layers increases the film thickness and the amount of catalyst available. Thus, if control by reaction kinetics is assumed, the observed increase in  $I_c/I_d$  for catalytic reduction of oxygen and an increased yield of styrene oxide is predicted as film thickness increases. However, an increase in the number of layers of catalyst increases the probability that the protein closest to the electrode will become less available to reactant molecules due to decreased permeation, and may thus limit the rate of reaction.<sup>[23]</sup> Competition between increased protein loading and decreased mass transport efficiency leads to a maximum in catalytic efficiency for oxygen reduction as film thickness increases. For styrene epoxidation, the most efficient catalysis is found with the thinnest films. In this case, however, it is practically useful to employ thicker films in order to obtain larger material yields (Table 1). Similar mass transport limiting effects of thickness on voltammetric catalytic efficiency and turnover rates were found in the conversion of dibromocyclohexane to cyclohexene by films of cobalt corrin-polylysine covalently bound to PG electrodes.<sup>[24]</sup>

### Influence of pH

The pH value of the external solution strongly influenced redox potential (Figures 4 and 5). The pH conditions had a small influence on CV peak separation, which is inversely related to electron transfer efficiency<sup>[9]</sup> and is also influenced by redox-coupled conformational changes.<sup>[17]</sup> The amount of electroactive protein in the films did not depend on pH value. The reversible changes of  $E^{\circ'}$  and  $\Delta E_p$  values with changing pH level clearly show that the redox properties of the proteins in the films are controlled by the pH value of the external buffer. The linear plots of  $E^{\circ'}$  against pH between pH 3 and pH 11 (Figure 5) had slopes close to the theoretical value of  $-59 \text{ mVpH}^{-1}$  expected at 25 °C for reversible proton-coupled electron transfer. The charged outer layers of the films should not be influenced to any great extent by pH changes, especially since 0.1 M NaCl was used in all buffers to maintain nearly constant ionic strength so Donnan membrane potential effects should not be a major factor in the

pH dependence of the  $E^{\circ'}$  value. We can therefore rationalize the  $E^{\circ'}$ /pH dependence of Mb and cyt P450<sub>cam</sub> reduction in these films as coupled with a proton transfer throughout the entire pH range.

The  $E^{\circ'}$ /pH behavior in the films evaluated here was very different from that of Mb and cyt P450<sub>cam</sub> in films of insoluble lipids and surfactants. In these lamellar liquid crystal films, linearity was found between pH 4.6 and pH 11 for Mb and between pH 6 and pH 11 for cyt P450<sub>cam</sub>, with slopes close to 59 mVpH<sup>-1</sup>, which suggests proton-coupled electron transfer within these pH ranges.<sup>[25–27]</sup> At lower pH values, however, Mb in the lipid films had an  $E^{\circ'}$  value nearly independent of pH conditions, and the slope for cyt P450<sub>cam</sub> was about half that at higher pH values. These results were correlated with protonation and partial denaturation of the proteins in the low-pH range, as confirmed by IR and visible absorption spectroscopy.<sup>[25, 27]</sup> Furthermore, the amount of electroactive proteins in the lipid films depended strongly on pH value, which is not the case in the polyion films. We recently obtained circular dichroism and visible absorbance spectra and voltammetric data on layered, cross-linked Mb/PSS films<sup>[28]</sup> that showed that Mb retains a near-native conformation and good catalytic activity for reduction of H<sub>2</sub>O<sub>2</sub>, O<sub>2</sub>, and trichloroacetic acid at pH values as low as 2. That is, the structure of the polyion–protein films appears to impart remarkable protection against acid denaturation of the protein. This could explain the linear  $E^{\circ'}$ /pH behavior extending into the low pH range. If the protein is held in the same conformation at low pH values as in neutral solutions, then the one-proton/one-electron reduction mechanism should remain the same. Thus,  $E^{\circ'}$  should, as observed (Figure 5), shift with changing pH at the same rate throughout the entire pH range.

Typical bell-shaped activity/pH profiles with maxima at close to physiological pH values were found both for H<sub>2</sub>O<sub>2</sub> driven styrene oxidation catalyzed by Mb and cyt P450<sub>cam</sub> and for electrolytic styrene oxidation catalyzed by cyt P450<sub>cam</sub> (Figures 9 and 10). Furthermore, the maximum turnover rate for cyt P450<sub>cam</sub> is in the same range as the turnover rate of 10 hr<sup>-1</sup> at 4 °C for the natural dissolved putidaredoxin–cyt P450<sub>cam</sub> system. The slightly higher value in solution is probably a consequence of full utilization of the dissolved enzyme, compared to the films, which show the influence of mass transport limitations even for two layers of protein.

The pH-dependent results are reasonable in view of the several steps in the cyt P450 catalytic mechanism that utilize protons,<sup>[12, 13, 29, 30]</sup> and these results support the view<sup>[2–6]</sup> that enzymes in these films have catalytic functionality similar to enzymes in solution. The amount of hydrogen peroxide was the same in all these experiments (about 10 mM). On the other hand, for electrolytic styrene oxidation catalyzed by Mb, turnover rate decreased with increasing pH value but was also correlated with the amount of hydrogen peroxide produced by catalytic reduction of oxygen (see Scheme 1) during the reaction (Figure 9). Thus, we tentatively conclude that, despite the conformational stabilization of the protein at low pH values described above, protonation–deprotonation reactions essential to catalytic activity occur in the films in a fashion consistent with established ideas of enzyme kinetics.

## Summary and Conclusions

We have reported, for the first time, the influence of polyion material, film thickness, and pH value on the electrochemical and catalytic activity of polyion–protein films constructed layer-by-layer with Mb and cyt P450<sub>cam</sub>. Synthetic organic polyions such as PSS supported the best catalytic and electrochemical performance and facilitated electron transport through 70 nm films (Figure 3). Electrons can be transported relatively efficiently over this film thickness, and over 320 nm with SiO<sub>2</sub> as the polyion. However, much thinner films (ca. 12–25 nm) gave the highest rates for catalytic electrochemical or hydrogen peroxide driven epoxidation of styrene. Classical bell-shaped activity/pH profiles (Figures 9 and 10), turnover rates at 4 °C similar to those in solution, and products of cyt-P450-catalyzed drug oxidation the same as those found previously<sup>[10]</sup> suggest that this approach is applicable to turnover rate studies of heme enzymes, and other enzymes as well. A major advantage is the very small amount of protein required: only 1.6 nmol or 75 µg P450<sub>cam</sub> was required for each turnover rate experiment.

## Experimental Section

**Materials:** Lyophilized horse-heart myoglobin (Mb, MW 17 400) from Sigma was dissolved in acetate buffer (10 mM, pH 5.2) and filtered through YM30 (Amicon, 30 000 MW cut-off) filters.<sup>[31]</sup> Cytochrome P450<sub>cam</sub> (MW 46 500) was from *Pseudomonas putida* expressed in *Escherichia coli* DH52α containing P450<sub>cam</sub> cDNA and was isolated and purified as described previously.<sup>[27]</sup> Putidaredoxin was obtained and purified as described previously.<sup>[32]</sup> Polyions were: PSS, average MW 70 000, Aldrich; PDPA, MW 200 000–350 000, Aldrich; PEI, average MW 70 000, Wako, Japan; calf thymus double-stranded DNA, Sigma (type XV). Silica nanoparticles of average diameter 45 nm in pH 10 solution were from Nissan Kagaku, Japan. Styrene, styrene oxide, and benzaldehyde were from Sigma. The buffers used were: acetate (0.05 M, pH 4.0–5.5); citrate (0.05 M, pH 3.0–7.0); tris(hydroxymethyl)aminomethane (Tris) (0.05 M, pH 7.0–9.0); borate (0.05 M, pH 9.0–10.0); phosphate (0.05 M, pH 1.5–3.0, 7.0–8.0, and 11.0); all contained NaCl (0.1 M). Water was purified to a specific resistance of approximately 18 µΩ cm<sup>-1</sup>. All other chemicals were reagent grade.

**Film assembly:** Multilayer films were grown on basal plane pyrolytic graphite (Advanced Ceramics) disk electrodes and on gold-coated quartz crystal microbalance resonators (9 MHz, AT-cut, International Crystal Mfg. Co., gold area 0.16 cm<sup>2</sup>). Prior to film assembly, the PG electrodes were abraded with 600-grit SiC paper (Buehler) while flushing with water, then roughened on medium Crystal Bay emery paper (PH 3M 001K) and washed extensively. The electrochemically determined surface area was 0.21 cm<sup>2</sup>.<sup>[33]</sup> For electrolyses, films were grown on carbon cloth (Zoltek Corp, 1.5 × 6.0 cm) with an active electrochemical area of 230 cm<sup>2</sup>. Clean Au-coated QCM resonators were coated before film formation by immersion in 3-mercaptopropionic acid (0.3 mM) and 3-mercaptop-1-propanol (0.7 mM) in ethanol to give a uniform negative surface that mimics graphite.<sup>[20]</sup>

Aqueous solutions for film construction were PSS or PDPA (3 mg mL<sup>-1</sup>), PEI (2 mg mL<sup>-1</sup>), DNA (1 mg mL<sup>-1</sup>), and SiO<sub>2</sub> (0.02 M, pH 9.0) nanoparticle solutions. Cyt P450<sub>cam</sub> (pI = 4.6)<sup>[12]</sup> was adsorbed at 1 mg mL<sup>-1</sup> in Tris buffer (10 mM, pH 7.4), in which it is negatively charged, while Mb (pI ≈ 7)<sup>[34]</sup> was adsorbed at 3 mg mL<sup>-1</sup> in acetate buffer (10 mM, pH 5.5), in which it is positively charged. Films were grown by repeated 20-min adsorption to achieve saturation<sup>[6]</sup> of



negative and positive polyions or proteins in alternate cycles to give films denoted as (Mb/polyion)<sub>n</sub> and (Cyt P450<sub>cam</sub>/polyion)<sub>n</sub> and (Mb/SiO<sub>2</sub>)<sub>n</sub>, where *n* is the number of protein/polyion bilayers. Films were washed with water and dried under a stream of nitrogen after each bilayer adsorption step before voltammetric or QCM analyses. In some cases, the adsorption of polyions was carried out from salt solutions and is denoted with salt concentration (for example, PSS (0.5 M NaCl)). For (Mb/SiO<sub>2</sub>)<sub>n</sub> films, the first layer of SiO<sub>2</sub> was adsorbed on a PSS/PDDA precursor bilayer adsorbed on the electrode. The first layer on the rough PG or carbon cloth in all the different film architectures was always polyion rather than protein, to avoid the denaturation and low activity possible with an initial protein layer.<sup>[21]</sup>

**Quartz crystal microbalance:** QCM resonators (9 MHz, AT-cut, International Crystal Mfg. Co.) covered by 100 nm evaporated gold electrodes (0.16 cm<sup>2</sup>) were used with a QCM from USI Systems, Japan. Films were prepared on resonators as described above. The resonator was immersed in a given adsorbate solution, washed, and dried in a stream of nitrogen, and the frequency change was measured at ambient temperature.

**Voltammetry:** A CHI 430 electrochemical workstation was used for cyclic voltammetry and controlled potential electrolysis. The three-electrode voltammetric cell contained a saturated calomel reference electrode (SCE), platinum wire counter-electrode, and a PG disc working electrode. Ohmic drop was compensated to < 0.5 mV by the CHI 430. Prior to CV, solutions were purged with purified nitrogen, unless otherwise noted, and the temperature was 25 ± 0.2 °C.

**Epoxidation of styrene:** Catalytic oxidation of styrene was performed with films made on both sides of carbon cloth electrodes. Electrolyses were done at an applied potential of −0.6 V with respect to SCE at 4 °C in a divided cell equipped with a spectroscopic carbon-rod counter electrode and an SCE reference, with compartments separated by an agar–NaCl salt bridge. Oxygen was passed through the reaction solution for the first 20 min, followed by oxygen blanketing above the solution for the remainder of the reaction. Alternatively, hydrogen peroxide was added to the cell without electrolysis with the vessel open to air. After 1 hr, 10-mL samples were extracted with hexane and the extract was analyzed by gas chromatography. The chromatographic assay and the estimation of H<sub>2</sub>O<sub>2</sub> was described previously.<sup>[6, 7]</sup> All reactions were run in triplicate. Oxidation of styrene with enzyme dissolved in solution was done at 4 °C by a published method,<sup>[19]</sup> with the molar ratio cyt P450<sub>cam</sub>/putidaredoxin/putidaredoxin reductase 1:8:2, and NADH (1 mM).

*This work was supported by US Public Health Service grant no. ES03154 from the National Institute of Environmental Health Sciences (NIEHS) at the National Institutes of Health (NIH). The contents are solely the responsibility of the authors and do not necessarily represent the official views of the NIEHS, NIH.*

[1] Y. M. Lvov, G. Decher, *Crystallogr. Rep.* **1994**, 39, 628–647.

[2] Y. Lvov in *Protein Architecture: Interfacing Molecular Assemblies and Immobilization Biotechnology* (Eds.: Y. Lvov, H. Möhwald), Marcel Dekker, N.Y., **2000**, pp. 125–167.

- [3] Y. Lvov in *Handbook Of Surfaces And Interfaces Of Materials, Vol. 3, Nanostructured Materials, Micelles and Colloids* (Ed.: R. W. Nalwa), Academic Press, San Diego, **2001**, pp. 170–189.
- [4] K. Ariga, T. Kunitake in *Protein Architecture: Interfacing Molecular Assemblies and Immobilization Biotechnology* (Eds.: Y. Lvov, H. Möhwald), Marcel Dekker, N.Y., **2000**, pp. 169–191.
- [5] Y. Lvov, B. Munge, O. Giraldo, I. Ichinose, S. L. Suib, J. F. Rusling, *Langmuir* **2000**, 16, 8850–8857.
- [6] Y. M. Lvov, Z. Lu, J. B. Schenkman, X. Zu, J. F. Rusling, *J. Am. Chem. Soc.* **1998**, 120, 4073–4080.
- [7] X. Zu, Z. Lu, Z. Zhang, J. B. Schenkman, J. F. Rusling, *Langmuir* **1999**, 15, 7372–7377.
- [8] J. F. Rusling, *Electroactive and Enzyme-Active Protein-Polyion Films Assembled Layer-by-Layer in Protein Architecture: Interfacing Molecular Assemblies and Immobilization Biotechnology* (Eds.: Y. Lvov, H. Möhwald), Marcel Dekker, N.Y. **2000**, pp. 337–354.
- [9] J. F. Rusling, Z. Zhang in *Handbook Of Surfaces And Interfaces Of Materials, Vol. 5, Biomolecules, Biointerfaces, and Applications* (Ed.: R. W. Nalwa), Academic Press, **2001**, pp. 33–71.
- [10] S. Joseph, J. F. Rusling, Y. M. Lvov, T. Freidberg, U. Fuhr, *Mol. Pharmacol.*, submitted.
- [11] J. B. Schenkman, I. Jansson, Y. Lvov, J. F. Rusling, S. Boussaad, N. J. Tao, *Arch. Biochem. Biophys.* **2001**, 385, 78–87.
- [12] *Cytochrome P450* (Ed.: P. R. Ortiz de Montellano), Plenum, New York, **1995**, pp. 159–206.
- [13] *Cytochrome P450* (Eds.: J. B. Schenkman, H. Greim), Springer, Berlin, **1993**.
- [14] Y. Lvov, K. Ariga, I. Ichinose, T. Kunitake, *J. Am. Chem. Soc.* **1995**, 117, 6117–6123.
- [15] R. W. Murray in *Electroanalytical Chemistry* (Ed.: A. J. Bard), Marcel Dekker, New York, **1984**, Vol. 13, pp. 191–368.
- [16] A. M. Bond, *Modern Polarographic Methods in Analytical Chemistry*, Marcel Dekker, New York, **1980**, pp. 29–30.
- [17] A. El Kasmi, M. C. Leopold, R. Galligan, R. T. Robertson, S. S. Saavedra, K. El Kacemi, E. F. Bowden, *Electrochem. Commun.* **2002**, 4, 177–181.
- [18] a) P. R. Ortiz de Montellano, C. E. Catalano, *J. Biol. Chem.* **1985**, 260, 9265–9271; b) S. I. Rao, A. Wilks, P. R. Ortiz de Montellano, *J. Biol. Chem.* **1993**, 268, 803–809.
- [19] J. A. Frutet, J. R. Collins, D. L. Camper, G. H. Loew, P. R. Ortiz de Montellano, *J. Am. Chem. Soc.* **1992**, 114, 6987–6993.
- [20] L. Zhou, James F. Rusling, *Anal. Chem.* **2001**, 73, 4780–4786.
- [21] H. Ma, N. Hu, J. F. Rusling, *Langmuir* **2000**, 16, 4969–4975.
- [22] G. Decher, *Science* **1997**, 227, 1232–1237.
- [23] C. P. Andrieux, J. M. Savéant in *Molecular Design of Electrode Surfaces, Techniques of Chemistry Series Vol. 22* (Ed.: R. W. Murray), Wiley, New York, **1992**, pp. 207–270.
- [24] C. J. Campbell, C. K. Njue, B. Nuthakki, J. F. Rusling, *Langmuir* **2001**, 17, 3447–3453.
- [25] A.-E. F. Nassar, Z. Zhang, N. Hu, J. F. Rusling, T. F. Kumosinski, *J. Phys. Chem. B* **1997**, 101, 2224–2231.
- [26] J. F. Rusling, *Acc. Chem. Res.* **1998**, 31, 363–369.
- [27] Z. Zhang, A.-E. F. Nassar, Z. Lu, J. B. Schenkman, J. F. Rusling, *J. Chem. Soc. Faraday Trans.* **1997**, 93, 1769–1774.
- [28] V. Panchagnula, C. V. Kumar, J. F. Rusling, *J. Am. Chem. Soc.* **2002**, 124, 12515–12521.
- [29] S. G. Sligar, I. C. Gunsalus, *Biochemistry* **1979**, 18, 2290–2295.
- [30] D. L. Harris, G. H. Loew, *J. Am. Chem. Soc.* **1998**, 120, 8941–8948.
- [31] A.-E. F. Nassar, W. Willis, J. F. Rusling, *Anal. Chem.* **1995**, 67, 2386–2392.
- [32] Z. Lu, Y. Lvov, I. Jansson, J. B. Schenkman, J. F. Rusling, *J. Coll. Interface Sci.* **2000**, 224, 162–168.
- [33] J. F. Rusling, L. Zhou, B. Munge, J. Yang, C. Estavillo, J. B. Schenkman, *Faraday Discuss.* **2000**, 116, 77–87.
- [34] Y. Goto, A. L. Fink, *J. Mol. Biol.* **1990**, 214, 803–805.

Received: June 25, 2002 [F443]